Isobaric-Analog States in Sc^{49}†

K. W. JONES
Brookhaven National Laboratory, Upton, New York

AND

J. P. SCHIFFER, L. L. LEE, JR.,* A. MARINOV,‡ AND J. L. LERNER
Argonne National Laboratory, Argonne, Illinois

(Received 11 January 1966)

Cross sections for the elastic scattering of protons by Ca^{48} have been measured at laboratory angles of 90°, 120°, and 160° for bombarding energies from 1.3 to 7.0 MeV. Prominent anomalies were observed in the excitation curves at c.m. proton energies of 1.935±0.003, 1.945±0.003, 3.86±0.03, 5.952±0.005, and 5.994±0.005 MeV. These anomalies indicate the positions of states in the compound nucleus Sc^{49} that are isobaric analogs of the ground state and excited states of Ca^{49}. An analysis of these data and a comparison with the $Ca^{48}(d,p)Ca^{49}$ results are presented. A value of 7.090±0.006 MeV for the Ca^{49}-Sc^{49}, Coulomb energy difference is obtained from the observed proton bombarding energy for the ground-state analog. All the known Coulomb energies for the odd Ca and Sc isotopes have been analyzed in terms of a simple model using single-particle wave functions in a Woods-Saxon well, and are interpreted in terms of charge radii.

I. INTRODUCTION

ISOBARIC-analog resonances[1,2] have so far been studied mostly in rather heavy nuclei. Some analog states have been observed by the (p,d) reaction[3] for nuclei around $A \approx 50$–60 and by the (He^3,d) reaction in the same region of nuclei[4] as well as in the Ca isotopes.[5,6] The nucleus Ca^{48} seems to form a closed shell for both protons and neutrons and the low-lying energy levels of both Ca^{49} (Ref. 7) and Sc^{49} (Ref. 8) seem to be of particularly simple single-particle character. In addition, Ca^{48} is the lightest stable nucleus with a neutron excess of 8 (Z component of isobaric spin $T_Z=4$). The low-lying states in Ca^{49} ($T=\frac{9}{2}$, $T_Z=\frac{9}{2}$) will have their analogs as highly excited compound-nucleus resonances in Sc^{49} ($T=\frac{9}{2}$, $T_Z=\frac{7}{2}$). In the present paper[9] we report an experimental study of these resonances.

II. EXPERIMENTAL METHOD

The experiment was carried out with proton beams from the Argonne 4.5-MeV electrostatic accelerator and tandem Van de Graaff. The 4.5-MeV accelerator was used for the investigation of the low-energy region below 3.3 MeV and the tandem for the region above 3.3 MeV. The energy spread of both proton beams was less than 0.05% with an uncertainty in the energy calibration of ±0.1%.

The source material for the Ca^{48} targets was $CaCO_3$

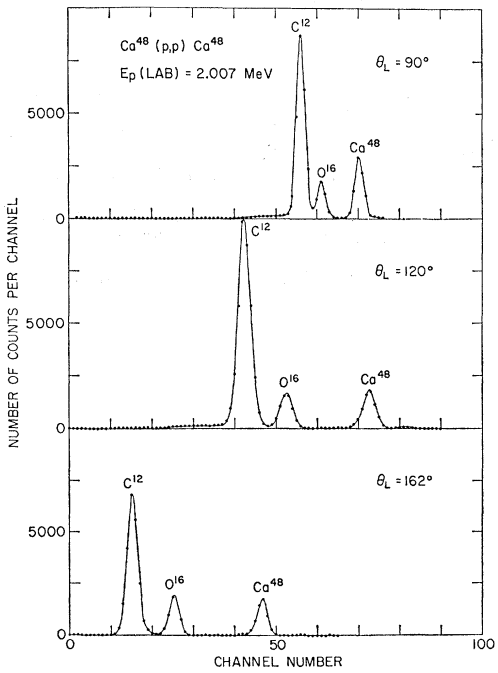

FIG. 1. Pulse-height spectra obtained at a bombarding energy of 2.007 MeV at laboratory angles of 90°, 120°, and 162°. Protons scattered from the Ca^{48} are clearly resolved from those scattered by the carbon foil and the oxygen contaminant. Spectra obtained at other energies were similar to the ones shown here.

† Work performed under the auspices of the U. S. Atomic Energy Commission.

* Now at State University of New York, Stony Brook, New York.

‡ Now at Hebrew University, Jerusalem, Israel.

[1] J. D. Fox, D. Robson, and C. F. Moore, Phys. Rev. Letters **12**, 198 (1964).

[2] L. L. Lee, Jr., A. Marinov, and J. P. Schiffer, Phys. Letters **8**, 352 (1964).

[3] R. Sherr, B. F. Bayman, E. Rost, M. E. Rickey, and C. G. Hoot, Phys. Rev. **139**, B1272 (1965).

[4] A. G. Blair and D. D. Armstrong, Phys. Rev. **140**, B1567 (1965).

[5] J. J. Schwartz and W. P. Alford, Bull. Am. Phys. Soc. **10**, 479 (1965) and (private communication).

[6] D. M. Sheppard, H. A. Enge, and H. Y. Chen, Bull. Am. Phys. Soc. **10**, 25 (1965); R. Bock, H. H. Duhm, and R. Stock, Phys. Letters **18**, 61 (1965).

[7] E. Kashy, A. Sperduto, H. A. Enge, and W. W. Buechner, Phys. Rev. **135**, B865 (1965).

[8] J. R. Erskine, J. P. Schiffer, and A. Marinov, Bull. Am. Phys. Soc. **9**, 80 (1964); J. R. Erskine, A. Marinov, and J. P. Schiffer, Phys. Rev. **142**, 633 (1966).

[9] A preliminary report of this work was given by K. W. Jones, A. Marinov, L. L. Lee, Jr., and J. P. Schiffer, Bull. Am. Phys. Soc. **10**, 479 (1965).

enriched to 78% Ca^{48}, obtained from the Oak Ridge National Laboratory. After conversion to the chloride, the sample was placed in a small quartz oven[10] adjacent to the ion source of the Argonne research electromagnetic isotope separator (AREMIS). The Ca^{48} beam was isolated by suitable apertures, retarded[10] to 500 V, and allowed to collect on a 40-$\mu g/cm^2$ carbon film. Since the nearest stable calcium isotope is two mass units away and of low abundance, the isotopic purity of the targets should be very high; it is estimated the concentration of other calcium isotopes in the targets was less than 0.1%. The area covered by the deposit was roughly

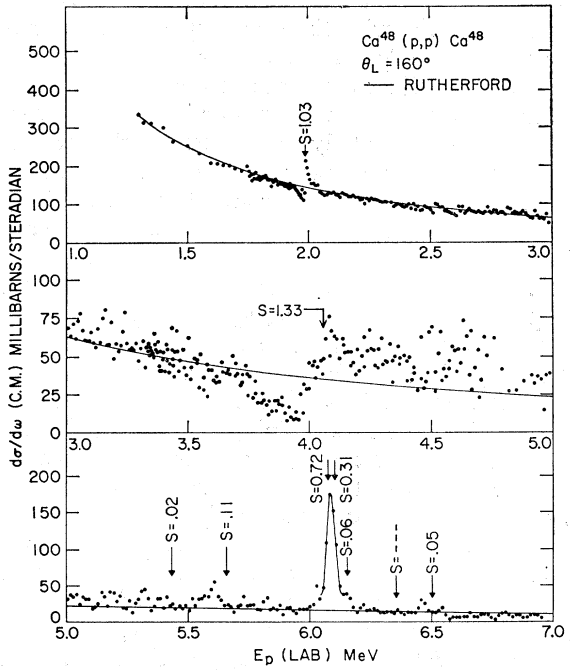

FIG. 2. Excitation curve for $Ca^{48}(p,p)Ca^{48}$, obtained at a laboratory angle of 160°. The anomaly at $E_p=1.989$ MeV is identified as the analog of the C^{49} ground state and the arrows mark the positions of the analog states based on this identification and the spacings of the Ca^{49} states found by Kashy *et al.* (Ref. 7). Spectroscopic factors S found by Kashy *et al.* are also indicated. Analog states are expected to be prominent if they correspond to Ca^{49} states that have a large spectroscopic factor. The statistical uncertainties are approximately the size of the points.

circular, approximately 4.5 mm in diam. The estimated thickness of the target (about 10 $\mu g/cm^2$) corresponds to an energy loss of about 1 keV for a 2-MeV proton.

The protons were detected with silicon surface-barrier detectors placed at 90°, 120°, and 160° to the incident proton beam. The angular width subtended by the counters was about ±3°. The pulse-height spectra taken at 2.007 MeV are shown in Fig. 1. Similar spectra were obtained over the entire range of energy covered. For the actual measurements, a single-channel analyzer was set on the Ca^{48} peak and the number of counts was

[10] J. Lerner, Nucl. Instr. Methods (to be published in 1966 as part of the Proceedings of the Aarhus Conference).

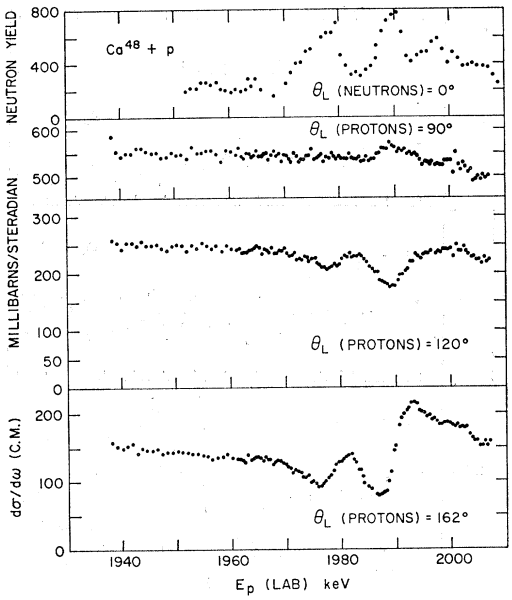

FIG. 3. Detailed excitation curves for $Ca^{48}+p$ over the region of the analog state which corresponds to the Ca^{49} ground state. It can be seen that the strength of the analog state is shared between at least two states and that there is some weak evidence for further structure around 2.000 MeV. The statistical uncertainties are about the size of the points.

recorded on a scaler. The pulse-height spectra were continuously monitored and the bias settings were checked frequently with a multichannel analyzer.

A scale of absolute cross section was established for the data below 3.3 MeV by normalizing the excitation curves to the Rutherford scattering cross section in the interval from 1.3 to 1.5 MeV. The 160° data shown in Fig. 2 were normalized to the low-energy data at 3.3 MeV.

Some measurements of the yield of neutrons from the $Ca^{48}(p,n)Sc^{48}$ reaction were made for a laboratory angle of 0°. A standard long counter was used to detect the neutrons. No effort was made to establish a scale of absolute cross section.

III. EXPERIMENTAL RESULTS

The excitation curves obtained in the present experiment are shown in Figs. 2–5. Figure 2 shows the excitation curve obtained at 160° over the entire energy range. The anomaly at about 2 MeV is identified as the $T=\frac{9}{2}$ isobaric analog of the Ca^{49} ground state. The states marked at higher energies are based on the position of the ground state and the known spacing of energy levels in Ca^{49}. It can be seen that the other two prominent anomalies can also be identified as isobaric analogs of states in Ca^{49} and that some plausible identifications can be made for the weaker anomalies. The regions in which the prominent anomalies occur are shown in more detail in Figs. 3–5.

One other measurement which is relevant to the

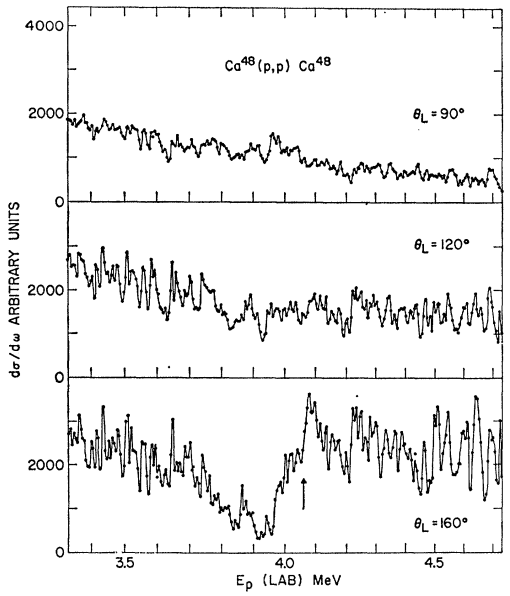

FIG. 4. Excitation curves for $Ca^{48}(p,p)Ca^{48}$ over the analog state that corresponds to the first excited state of Ca^{49}. An arrow indicates the position of the state as expected from the position of the Ca^{49} ground-state analog and the energy spacing of the ground state and first excited state in Ca^{49} measured by Kashy *et al.* (Ref. 7). Statistical uncertainties are comparable to the size of the points. The rapid fluctuations in the excitation curves are caused by the excitation of narrow states with $T=\frac{7}{2}$.

position of the analog of the Ca^{49} ground state has been made by El-Nadi *et al.*[11] They measured the yield of 0.37-MeV gamma rays from the $Ca^{48}(p,n\gamma)Sc^{48}$ reaction as a fair indication of the total neutron cross section. They apparently observe the analog of the ground state at a c.m. energy of about 1.913 MeV, which is about 27 keV lower than the energy found here. The source of this discrepancy is not known.

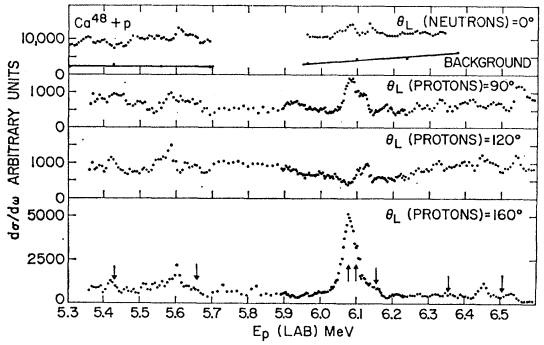

FIG. 5. Excitation curves for $Ca^{48}+p$. The analog states corresponding to the second and higher excited states of Ca^{49} should be seen in the region shown. Arrows mark the positions of analog states calculated from the position of the Ca^{49} ground-state analog and the energy spacings of states in Ca^{49} measured by Kashy *et al.* (Ref. 7). Statistical uncertainties are comparable to the size of the points.

[11] L. M. El-Nadi, O. E. Badauy, A. El-Sourogy, D. A. E. Darwich, and V. Y. Gontchar, Nucl. Phys. **64**, 449 (1965).

IV. ANALYSIS AND DISCUSSION

While the identification of the analog states was straightforward for those which produced large anomalies (i.e., large proton reduced widths), a further check was made by verifying that the shape of the resonance was indeed that produced by a proton with the proper orbital angular momentum l to excite the analog state with spin and parity J^π. The shapes of single-particle resonances can be generated easily and quickly by use of an optical-model program.[12] In the present experiment it is expected from the stripping results[7] that the analogs of the ground state and first excited state of Ca^{49} will be formed in Sc^{49} by p-wave protons. If an optical potential with the usual depth is used for the calculation, the $2p$ states are bound. It was therefore necessary to adjust the depth of the real potential to get the $2p_{3/2}$ resonance at the proton bombarding energy observed experimentally. Estimates of the expected proton width for the observed states are also obtained in a crude fashion from this calculation.[13] If the imaginary part of the optical potential is set equal to zero, then the calculated width of the single-particle state must be just the same as the single-particle proton width Γ(s.p.). The expected single-particle proton width Γ_a(s.p.) of the analog state is found[14] by dividing Γ(s.p.) by $(2T+1)$. Here T is the isobaric spin of the target so that $2T+1=9$. If the measured proton width Γ_p found from the data is divided by Γ_a(s.p.) the spectroscopic factor for the (d,p) reaction is obtained and can be compared with the spectroscopic factors found in a distorted-wave analysis of stripping data.

The shapes for $p_{3/2}$, $p_{1/2}$, $f_{5/2}$, and $g_{9/2}$ resonances (Fig. 6) were found in the optical-model calculation and qualitatively verify the identification of the strong anomalies in the excitation curve as analog states with l values consistent with the (d,p) work. The calculations used a real well depth of about 47 MeV and a spin-orbit strength of 10.5 MeV with radii equal to 4.54 F and a diffusivity of 0.6 F. The imaginary part of the potential was set equal to zero so that values of Γ_a(s.p.) were also obtained. The well depths were adjusted slightly to place each state at about the observed bombarding energy. It should be remembered that the shapes shown in Fig. 6 are for the case $\Gamma_p=\Gamma_a$(s.p.) and that this condition is not true experimentally for the $f_{5/2}$-$g_{9/2}$ doublet.

While a check on the l values and the spin-parity of the states can be reasonably made from the shapes of the anomalies, the data must be further examined in order to obtain values for the resonant energies, total widths, and proton partial widths.

[12] All calculations with a Woods-Saxon potential were performed by use of the optical-model code ABACUS kindly supplied to us by E. Auerbach.

[13] J. P. Schiffer, Nucl. Phys. **46**, 246 (1963).

[14] D. Robson, Phys. Rev. **137**, B535 (1965); P. Richard, C. F. Moore, D. Robson, and J. D. Fox, Phys. Rev. Letters **13**, 343 (1964).

The analysis of the Ca^{49} ground-state analog is complicated by the apparent sharing of the strength between two states 10 keV apart, as is shown in Fig. 3. The shape of each state at all three angles is consistent with formation by $l=1$ protons and we assume that both have $J^\pi=\frac{3}{2}^-$, the spin of the ground state of Ca^{49}. The excitation curve at 162° was first analyzed by use of the graphical method of Laubenstein and Laubenstein.[15] At this energy, potential scattering amplitudes are negligible and only the Rutherford and resonant amplitudes need be considered. Since the neutron widths are not negligible, the resonant amplitude is decreased by a factor of Γ_p/Γ. Single-level phase shifts were used and E_R, Γ, and Γ_p/Γ were varied to get the best fit to each state at an energy close to the resonant energy. This procedure, of course, neglects interference between the two states of the same spin-parity and hence cannot be used to give an over-all fit to the data. To check that the parameters extracted by this procedure were reasonable, a two-level/two-channel formula for the cross section was used with these parameters to calculate the 162° cross section. The fit obtained is shown in Fig. 7. An ambiguity in this calculation involves the sign chosen for terms of the type $\Gamma_{1n}^{1/2}\Gamma_{2p}^{1/2}$ and $\Gamma_{1p}^{1/2}\Gamma_{2n}^{1/2}$

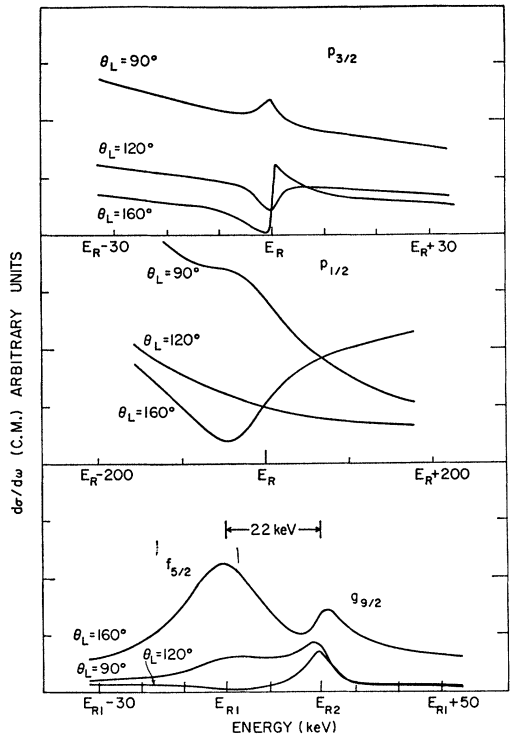

FIG. 6. Typical shapes for the analog states observed in this experiment. These curves were obtained from optical-model calculations making use of the parameters discussed in the text.

[15] R. A. Laubenstein and M. J. W. Laubenstein, Phys. Rev. **84**, 18 (1951); H. T. Richards, in *Nuclear Spectroscopy*, edited by F. Ajzenberg-Selove (Academic Press Inc., New York, 1960), Part A, p. 99.

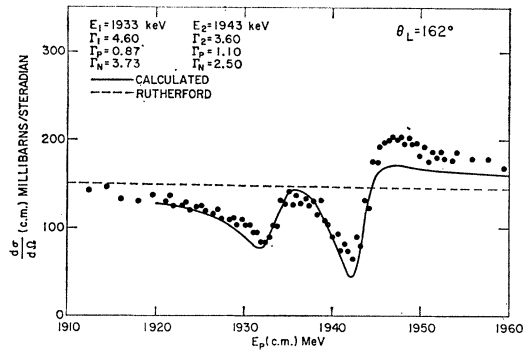

FIG. 7. Two-level/two-channel fit to the two resonances near 1940 keV on the assumption that they are both formed by p-wave protons and with $J^\pi=\frac{3}{2}^-$. The parameters used are shown in the figure.

and gives two different results. The fit chosen (Fig. 7) was the one that gave the best fit to the data. The fit obtained is quite good; while it might be improved by small variations of the chosen parameters, it was not felt that this improvement would be worth the effort. As a rough check on these values, the total (p,n) reaction cross section for the two states was computed. This can easily be done since $\Gamma=\Gamma_p+\Gamma_n$. Values of 44 and 52 mb were found for the 1935- and 1945-keV states, respectively, compared with the ~18 and ~20 mb estimated by El-Nadi *et al.*[11] It should also be pointed out that the values of Γ_p/Γ obtained are strongly influenced by the depth of the observed minima in the cross section. The estimated effect of the finite beam resolution for a triangular beam spread of 1 keV (full width at half-maximum) indicated that Γ_p/Γ should be about 10% greater than the Γ_p/Γ required to fit the actual cross section. Another calculation made use of the results of Hagedorn *et al.*,[16] who estimated the effects of a rectangular distribution of beam energies in reducing the sizes of the maxima and minima of isolated resonances. A beam width of 1 keV was found to change Γ_p/Γ by about 3%. Another factor that influences the depth of the observed minima is the finite target thickness. For the present case this is not known very well, but it is felt that it probably introduces a smaller correction than the finite spread in beam energy. The widths quoted in Table I were roughly corrected for the spread in beam energy. The energies quoted there are the average of two runs over this energy region. It should also be noted that the 120° data gave good agreement with the 162° data for the resonant energy. No effort was made to fit the data at 120°. At 90°, an incoherent peak can be seen clearly for the upper state but not for the lower state. An expanded plot of the data does give indication of an incoherent peak for the lower state and its size is consistent with that expected from the value of Γ_p/Γ of this state compared to the Γ_p/Γ of the upper state.

[16] F. B. Hagedorn, F. S. Mozer, T. S. Webb, W. A. Fowler, and C. C. Lauritsen, Phys. Rev. **105**, 219 (1957).

TABLE I. Summary of results. The column headings are discussed in the text.

c.m. energy, E_p Obs. (keV)	c.m. energy, E_p Calc.[a] (keV)	l	J^π	Γ (keV)	Γ_p (keV)	Γ_a(s.p.) (keV)	Spectroscopic factor $S=\Gamma_p/\Gamma_a$(s.p.)[b]	Spectroscopic factor From stripping[c]
1935± 3		1		4.6± 0.5	0.87± 0.2	3.1		
	(1940± 3)		$\frac{3}{2}^-$				0.64±0.07[d]	1.03
1945± 3		1		3.6± 0.5	1.10± 0.2	3.1		
3860±30	3968± 5	1	$\frac{1}{2}^-$	200 ±20	136 ±30	110	1.24±0.27	1.33
	5311± 8	2	$\frac{5}{2}^+$					0.02
(5486±10)	5535± 8	3	$\frac{5}{2}^-$					0.11
5952± 5	5945± 8	3	$\frac{5}{2}^-$	40 ± 5	24 ± 5	26	0.91±0.19	0.72
5994±10	5964± 8	4	$\frac{9}{2}^+$	25 ± 5	2.7 ± 0.8	9	0.31±0.09	0.31
(6028±10)	6018± 8	3	$\frac{5}{2}^-$					0.06
	6219±10							
(6319±10)	6362± 9	2	$\frac{5}{2}^+$					0.05
	7327±10							
	8035±15							

[a] Expected positions of analog levels from level spacings of Ca^{49}. These values, taken from Ref. 7, are based on the ground-state analog being at 1940±3 keV.
[b] The indicated uncertainties are from Γ_p only and do not include uncertainties in Γ_a(s.p.).
[c] Spectroscopic factor from the $Ca^{48}(d,p)Ca^{49}$ experiment of Ref. 7.
[d] Calculated from the sum of the proton widths for the 1935- and 1945-keV states.

There is some evidence for additional weak states in the region around incident energies of 2 MeV.

Analysis of the analog of the first-excited state is reasonably straightforward, the main complications being attributable to the higher proton energies involved. The data for this state at 90°, 120°, and 160° are shown in Fig. 4. There is evidence for fine structure from individual states or groups of states, presumably $T=\frac{7}{2}$, superimposed on the broad shape typical of a p-wave resonance, shown in Fig. 6. The first step in the analysis was to produce an averaged curve at 160° by drawing a reasonable average through this fine structure. This average curve was then used to obtain the parameters of the state. A first attempt to fit was made by calculating s-, p-, and d-wave potential phase shifts on the assumption of hard-sphere scattering. It was then not found possible to fit the cross sections at both the minimum and the maximum in the excitation curve with a single value of Γ_p/Γ. An optical-model calculation showed that the problem lay chiefly in the s-wave phase shift. Instead of carrying out elaborate calculations with the optical model, a simplified empirical procedure was used. The locus of the amplitudes for the maximum and minimum values of the cross section were used to deduce the value of Γ_p/Γ required to fit the data and the magnitude and phases of the resultant nonresonant amplitudes were adjusted to give the proper energy variation of the cross section. The resonant energy and total width were then adjusted to fit the curve of average cross section.

The remaining two strong states which were analyzed (Fig. 5) occur at 6.080 and 6.120 MeV. Referring again to Fig. 6 and remembering that the optical-model calculation is for $\Gamma_p=\Gamma_a$(s.p.), we see that the shapes of the curves are consistent with assignments of $f_{5/2}$ for the lower state and $g_{9/2}$ for the upper state. The resonant energy of the lower state can be found from the positions of the maximum at 90° and 160° and the minimum at 120°. Detailed analysis of the 120° data was not attempted since coherent and incoherent contributions from both resonant waves must be considered. At 160° the incoherent contributions can be neglected, but two resonant amplitudes must be considered. At 90°, however, the situation is fairly simple. Odd Legendre polynomials vanish and the only contribution from the $f_{5/2}$ resonance is an incoherent peak, which actually is the dominant feature of the excitation function. Since the incoherent peak must be symmetric, the low-energy shape of the peak was used on the high-energy side and subtracted from the observed data to obtain the contribution of the $g_{9/2}$ resonance. The two curves were then used to find the $g_{9/2}$ resonant energy and the total widths for the two states.

Extraction of the proton partial width is simple in principle, but is complicated here by the lack of absolute cross sections at 90°. The cross section was first estimated by assuming the nonresonant cross section could be adequately represented by the results of an optical-model calculation. For this computation, the potential used had a real well depth of 58 MeV, a spin-orbit well of 8 MeV, and an imaginary well which was a derivative of a Woods-Saxon shape with a strength of 11 MeV. A radius of 4.36 F was used for all the potentials with a diffuseness of 0.65 F for the real well and 0.47 F for the imaginary well. The Coulomb radius was 4.11 F. The cross section for the incoherent peak was then found and the value of Γ_p/Γ was extracted by use of the expression

$$\sigma(90)_{\text{inc}}=\lambda\!\!\!^{-2}[P_3'(\cos\theta)(\Gamma_p/\Gamma)\sin\delta_3^-]^2,$$

where δ_3^- is the $f_{5/2}$ phase shift. For the $g_{9/2}$ resonance the situation is somewhat more complicated because the resonant and nonresonant contributions are coherent. At 90° however, $P_4'(\cos\theta)$ is zero and there is no incoherent term, so that the value of Γ_p/Γ can easily be

found by use of the relation $|\sigma_{max}^{1/2}-\sigma_{min}^{1/2}|=\lambda(J+\frac{1}{2})\times P_L(\cos\theta)\Gamma_p/\Gamma$. The same relationship was also used to extract Γ_p/Γ for the $f_{5/2}$ state from the 160° data. At 160° the absolute cross section can be found within about ±30% from comparison with the low-energy data and the value of Γ_p/Γ is completely defined. A value was also found by normalizing the curve to the optical-model cross section found for 160°. The values found for Γ_p/Γ for the $f_{5/2}$ and $g_{9/2}$ resonances using the three different estimates for absolute-cross-section values were consistent within the estimated errors.

Structure within analog resonances, such as is shown in Figs. 2–4, has previously been studied in some detail for heavier nuclei and was attributed to interference between the analog resonance and a large number of states with lower T and the same spin-parity.[14] It is not clear how important this effect is in a relatively light nucleus such as Sc^{49} whose density of states with $T=\frac{7}{2}$ is relatively small, as is demonstrated by the experiment of El-Nadi *et al.*[11] In fact for Sc^{49}, as has been shown, the ground-state analog is split into only two states; and although the first-excited-state analog shows a great amount of fine structure, no evidence was found for the modulated interference effect described by Robson *et al.* Such results can be explained by lack of sufficiently high density and overlap for the states with $T=\frac{7}{2}$.

Our results are summarized and compared with other relevant data in Table I. The first column gives the observed center-of-mass proton energies for the analog resonances. Energies given in parentheses indicate resonances that are possible candidates for analog states, but which were so weak that detailed analysis was impossible. The expected energies for the analog states (second column) are based on a ground-state energy of 1940 keV and the known[7] spacing of levels in Ca^{49}. Values given for the orbital angular momentum l were those found by comparison with optical-model calculations and are consistent with stripping assignments. Our l values of course establish the parity of the levels, but the spin listed is that suggested by Kashy *et al.* The next columns give the total width and proton widths of levels found in the analysis that has just been described. Values for the expected single-particle proton width of the strong states are given as Γ_a(s.p.) and were obtained from the optical-model work previously described. The value of Γ_p/Γ_a(s.p.) is also tabulated since this is the spectroscopic factor for the level and should be equal to the spectroscopic factor S (last column) which is determined from the $Ca^{48}(d,p)Ca^{49}$ stripping experiment. The agreement between the properties of our resonances and those of their analog states in Ca^{49} is good, and, of course, gives confidence in the assignments that have been made. The stated uncertainties in Γ and Γ_p are estimates from the analysis. Uncertainties in the values of Γ_a(s.p.) are difficult to evaluate and no effort has been made to include uncertainties from that source in the values given for the spectroscopic factor. The sensitivity to the radius and diffuseness values chosen have been estimated by Schiffer[13] for the case of $Ca^{40}(p,p)Ca^{40}$.

TABLE II. Coulomb energy differences E_c.

Pair of nuclei	E_c (MeV)	$E_c(A/2Z)$ (MeV)
Ca^{41}-Sc^{41}	7.302[a]	7.243
Ca^{43}-Sc^{43}	7.230[b]	7.287
Ca^{45}-Sc^{45}	7.229[c]	7.401
Ca^{49}-Sc^{49}	7.090[d]	7.492

[a] The $Ca^{40}(d,p)Ca^{41}$ Q value was taken from T. A. Belote, A. Sperduto, and W. W. Buechner, Phys. Rev. **139**, B80 (1965). The $Ca^{40}(He^3,d)Sc^{41}$ Q value is that of Ref. 6.
[b] The $Ca^{42}(d,p)Ca^{43}$ Q value was taken from J. H. E. Mattauch, W. Thiele, and A. H. Wapstra, Nucl. Phys. **67**, 1 (1965). The $Ca^{42}(He^3,d)Sc^{43}$ analog-state Q value is that of Ref. 5.
[c] The $Ca^{44}(d,p)Ca^{45}$ Q value is that of J. H. E. Mattauch *et al.*, Ref. 6. The $Ca^{44}(He^3,d)Sc^{43}$ analog-state Q value was taken from Ref. 5.
[d] The $Ca^{48}(d,p)Ca^{49}$ Q value was taken from Ref. 7, the Sc^{49} analog-state energy is from the present experiment.

V. COULOMB ENERGIES

From the difference between the energies of the Ca^{49} ground state and its analog in Sc^{49}, we get a Coulomb-energy difference of 7.090±0.006 MeV, where an average weighted by the observed Γ_p was used for the average energy of the two states making up the Sc^{49} analog states. Comparing this value with the Coulomb-energy differences for other Ca-Sc isobars (Table II) shows that there are considerable fluctuations in the Coulomb energies even when multiplied by the usual $(A/2Z)^{1/3}$ to account for differing radii.[3]

We have performed a somewhat more sophisticated analysis of Coulomb energy differences in an attempt to interpret these differences. This analysis rests on the assumption that realistic wave functions for low-lying states can be calculated from a Woods-Saxon potential having the usual radial parameters found from elastic scattering.[17] The Coulomb energy difference can then be calculated by taking the Coulomb shift of such a wave function with a uniform charge distribution.[12]

This is perhaps best illustrated by a specific calculation of the Ca^{41}-Sc^{41} Coulomb energy difference. Taking $r_0=1.25$ F and $a=0.65$ F (using the standard notation for Woods-Saxon potentials), we find that the well depth required to give the observed binding for the $1f_{7/2}$ neutron single-particle state is 52.521 MeV. Next we calculate a proton state in the same well by use of a uniform charge distribution of radius $R_c=r_cA^{1/3}$ and find that $r_c=1.225$ F gives the observed Coulomb shift. The next single-particle state in Ca^{41} is the $2p_{3/2}$ state which is split into two components. For the single-particle energy of the $2p_{3/2}$ state in Ca^{41}, and likewise for that of the corresponding pair[18] in Sc^{41}, we take the

[17] F. G. Perey, Phys. Rev. **131**, 745 (1963).
[18] The real well depth was adjusted to fit the binding energy of each single-particle state. This gives us a slightly different potential for the $1f_{7/2}$ state than for the $2p_{3/2}$ state. A consistent potential could have been found by adjusting the spin-orbit part of the potential, but the difference in the wave function would have been negligible. The radial parameters of the well and the binding energy of the state are the most important parameters.

TABLE III. Summary of Coulomb energy differences. The column headings are discussed in the text.

Nuclei	State	E_b' (MeV)	E_b'' (MeV)	E_c' (MeV)	E_c'' (MeV)	r_c (F)	R_c (F)	E_c Obs. (MeV)	E_c Calc.[a] (MeV)
Ca^{41}-Sc^{41}	$1f_{7/2}$	8.360		7.302		1.225	4.189	7.302	
	$2p_{3/2}$	6.410		7.013		1.225		6.999	7.013
Ca^{43}-Sc^{43}	$1f_{7/2}$	7.929	9.912	7.164	7.268	1.235	4.293	7.230	
	$2p_{3/2}$	4.881	9.912	6.824	7.268	1.235		7.100	7.126
Ca^{45}-Sc^{45}	$1f_{7/2}$	7.419	9.742	7.125	7.256	1.185	4.183	7.229	
Ca^{49}-Sc^{49}	$2p_{3/2}$	5.150	9.262	6.701	7.139	1.136	4.129	7.090	

[a] Values of E_c for the first excited states in Ca^{41}-Sc^{41} and Ca^{43}-Sc^{43} were calculated from the R_c determined by use of the observed E_c for the ground-state pair.

center of gravity $E=\sum_i S_iE_i/\sum_i S_i$, where the S_i are the spectroscopic factors determined in stripping experiments. The observed Coulomb energy turns out to be 303 keV lower than for the $1f_{7/2}$ state. When the calculation is repeated with a $2p_{3/2}$ wave function in the Woods-Saxon well and with the same charge radius as was determined for the $1f_{7/2}$ state, the calculated Coulomb energy comes out 289 keV lower. In other words, *large fluctuations in Coulomb energies can arise from differences in the wave functions* of the states which are being considered. This method of calculation includes the effect of finite binding or, in the case of the unbound $2p_{3/2}$ state, the Thomas-Ehrmann shift in the resonance level.

The situation becomes a little more complicated in the other pairs of isobars. In Ca^{43}-Sc^{43}, for instance, it is necessary to include the Coulomb shift of all three particles. Since their binding energies are not the same, we cannot simply take the wave function of a neutron bound by the energy of the last neutron in Ca^{43}. Instead, we do one calculation using the binding energy E_b' of the last neutron of Ca^{43} and another one using the average binding energy E_b'' of the two neutrons in Ca^{42}. The Coulomb energy is then taken to be $E_c=\frac{2}{3}E_c''+\frac{1}{3}E_c'$, where E_c' and E_c'' are the Coulomb energies obtained for E_b' and E_b'', respectively. In this crude fashion we can calculate the Coulomb energy of Ca^{49} where $E_c=(8/9)E_c''+\frac{1}{9}E_c'$ with E_c'' calculated for $1f_{7/2}$ neutrons in Ca^{48} and E_c' for the $2p_{3/2}$ state with the actual binding of Ca^{49}.

Since the analog energy in Sc^{49} is weighted heavily by the Coulomb energy of the closed $1f_{7/2}$ shell, this explains the good agreement between the calculated and observed energies (Table I) for the analog states in Sc^{49}. The expectation that the fluctuations in energy would be about $\frac{1}{9}$ of those in Ca^{41}-Sc^{41} is consistent with our present results and also with the results[2] for Ni^{64} which also has $T=4$.

As an indication of the sensitivity to the choice of parameters in the Woods-Saxon well, it was observed in the calculations for the $1f_{7/2}$ state in Ca^{40} that $(\Delta R_c/R_c)/(\Delta a/a)=-0.042$ and $(\Delta R_c/R_c)/(\Delta R_0/R_0)=-1.43$. A consistent change in R_0 or a for all the nuclei would tend to alter the absolute values of R_c but not the relative ones. The values of E_c are known to approximately 10 keV. This causes an uncertainty of 0.5% in the charge radii.

The results of the calculations for all Ca-Sc pairs are summarized in Table III. While it is clear that these calculations are far from rigorous, they seem to reflect the qualitative trends in charge radii.

It is of interest to compare the differences between Ca^{44} and Ca^{40} charge radii as determined from muonic x-ray measurements[19] with the values obtained here. The ratio $R_c(Ca^{44})/R_c(Ca^{40})$ is perhaps the most meaningful to compare because it will be relatively insensitive to the particular shape assumed. The best value of this ratio from muonic x-ray measurements seems to be 1.009 ± 0.003 and the present experiment yields 0.998 ± 0.007. The comparison of absolute radii with those obtained from electron scattering[20] is not meaningful because of the different shapes used for the charge distribution.

ACKNOWLEDGMENTS

We are grateful to D. Robson and Dale D. Long for some computations which were very helpful in the analysis presented here and to P. D. Parker for calling the results of Ref. 16 to our attention. We would like to thank John McShane for his help with the experiment and computations, and J. R. Wallace and the operating crews of the Van de Graaff accelerators for their assistance.

[19] S. Raboy (private communication); R. C. Cohen, S. Devons, A. D. Kanaris, and C. Nissim-Sabat, Phys. Letters **11**, 70 (1964).
[20] D. G. Ravenhall, R. Herman, and B. C. Clark, Phys. Rev. **136**, B589 (1964).